Science Advances

AAAS

advances.sciencemag.org/cgi/content/full/3/12/e1701079/DC1

Supplementary Materials for

Resilience and efficiency in transportation networks

Alexander A. Ganin, Maksim Kitsak, Dayton Marchese, Jeffrey M. Keisler, Thomas Seager, Igor Linkov

Published 20 December 2017, *Sci. Adv.* **3**, e1701079 (2017)
DOI: 10.1126/sciadv.1701079

This PDF file includes:

Alternative approaches to model transportation

The extensive literature on transportation network modeling contains various alternative approaches to the one developed here.

Important group of graph theoretic approaches to system robustness and resilience look at the cascading failures propagation in spatially-embedded interdependent networks. For example, Berezin et al. (*38*) look at the cascading failures in coupled diluted lattices and determine a critical radius of localized percolation, which leads to the system's collapse. In work (*39*), the authors add recovery to probabilistic failure process in coupled spatial networks, and establish a phase space of probabilities, characterizing the up and down states of the two networks. Another study (*40*), which is particularly relevant to transportation, evaluates loads on nodes from their betweenness centralities. If after a localized removal of some nodes the betweenness of the surrounding nodes increases above a threshold proportional to their initial betweenness, an overload happens. This overload may then propagate across the network.

Widespread queueing models (*44*) consider traffic behavior in the vicinity of a certain location or section where the demand exceeds the available capacity (for example, at intersections). We do not utilize these models in this work for a number of reasons: i) we do not have information on the controlled and not controlled intersections; ii) to robustly formulate a queueing model we would need to consider temporal distribution of arrival and departure rates; iii) computationally, such models are more complex to solve for large networks (we consider networks of up to 39 791 nodes and 88 797 links (New York)) as it is necessary to account for the finite capacity of links and spillover effects, when a link may cause delays at connected links and increase wait times for traffic, which will not enter that link. Another approach is to evaluate delays from historical data and direct measurement (e.g. Google Maps). This approach is very accurate but requires extensive datasets and is not easily applicable to hypothetical scenarios, such as disruptions.

Gonzalez et al. (*41*) conducted a study on human mobility patterns and found that these patterns may be approximated by a random walk for which step size follows a truncated power law. Similar patterns were observed later by Cho et al. (*42*) and Calabrese et al. (*43*). In our work, however, we based our evaluation of the distance factor on the National Household Travel Survey as the scale of the mobility patterns reported is significantly different and covers travel of up to 10^4 kilometers (e.g., (*42*)). Mobility studies also have certain limitations. For example, among other characteristics, the first paper looks at distance distribution of travel and approximates it with a Lévy flight. We note, that in conditions of highly geometrically heterogeneous sources and destinations distributions, a random walk may be less accurate than models which account for this heterogeneity.

Mapping from OSM Foundation shapefiles to network nodes and links

The transportation topology is represented in Open Street Map (OSM) datasets as a table with rows defining segments of roads. Each row contains the following fields (fields marked as optional below may contain no data):

1) SHAPE – characterizes the road segment as a polyline defined by an ordered list of points coordinates;
2) NAME (optional) – contains the name of a road (e.g. street or highway name);
3) TYPE – specifies values showing the importance of a road (e.g. highway, trunk, primary, secondary, tertiary and others);
4) ONEWAY – represents whether a road segment is one way as a binary value (0 or 1);
5) MAXSPEED (optional) – provides the speed limit information for a particular road segment.

For simplicity and computational effectiveness, we do not consider minor residential streets and service roads in the analysis, thus limiting it to roads of 10 types, and assign a number of lanes to each type (table S1). Additionally, for each of the roads we calculate its length l_{ij} (using the shape of the polyline) and the free-flow speed (FFS). For non-ramps roads, the FFS is determined either as the value of the field MAXSPEED if it is non-zero, or as the average FFS across the whole network for roads of the same type and non-zero MAXSPEED. For ramps the FFS is determined as one third of the average FFS of the respective type roads. E.g., the FFS of highway ramps equals 1/3 of the average highway FFS. We analyze the effects it has on the results later in Supplementary Materials.

table S1. Mapping original OSM types to network link types and assignment of the number of lanes.

Link Type	OSM Dataset Type	Number of Lanes
High-speed (HS) highways	motorway	4
Highways	trunk	4
Primary roads	primary	3
Secondary roads	secondary	2
Tertiary roads	tertiary	1
HS highways ramps	motorway_link	2
Highways ramps	trunk _link	2
Primary ramps	primary _link	2
Secondary ramps	secondary_link	1
Tertiary ramps	tertiary_link	1

In the beginning of the network topology generation we create a map with keys corresponding to GPS coordinates, and values corresponding to nodes. For each of the points comprising the road polylines we first check if it should be included in the network based on the boundary polygon. A point is included if it is either inside the boundary polygon or within a certain distance from the polygon's border. In this study, the said distance was taken to be 25 miles (approximately 40 000 meters). If the point is included then we create a node and add it to the map using its coordinates (rounded to 10^{-5} decimal degrees) as the key, unless these coordinates are already in the map. Thus, all points of all road polylines have a corresponding node in the map. Finally, we connect all adjacent (as defined by the road polylines) nodes with either one directed link (if the road is one way) or two directed links (otherwise).

It is worth noticing that when a transportation system is represented as a network some nodes may be excluded. In particular, the nodes with only one neighbor, while able to serve as sources or destinations, do not contribute to the traffic carrying capacity of the system. For this reason, we removed all such nodes from the transportation network to simplify the model.

It is also possible to exclude the nodes with exactly two neighbors from the system. Such nodes typically appear for two reasons: i) due to our removal of residential and service roads from the network; ii) in the source datasets, as a way to differentiate between different road types or allowed speeds on the roads connected by such a node. To investigate the validity of removing nodes of degree 2 from our resulting network, in fig. S1 we present an analysis of characteristics of links, which are combined due to removal of such nodes. We look at differences in estimated speeds (fig. S1A) and numbers of lanes (fig. S1B). In total, across all 40 urban areas, 842 115 link pairs are combined. More than 97% pairs had speed differences between links less than 10 km/h and more than 99% had no differences in the estimated numbers of lanes. Thus, we conclude that the effect of the removal on the results is unlikely to be significant. We do the removal by connecting the two neighbors of 2-degree nodes directly as follows. Assume that node A has two neighbors: B_1 and B_2. Depending on the way the three nodes (B_1, A, and B_2) are connected we either disconnect nodes B_1 and B_2, or connect them with 1 or 2 directed links (in opposite directions). The links from B_1 to B_2 and from B_2 to B_1 are built in the same way so we only need to describe case B_1–B_2. The following two subcases are possible: i) there is a link from B_1 to A and from A to B_2; ii) there is no either or both of the links mentioned in i). In the first case, we can replace the two directed links B_1–A–B_2 with a single directed link B_1–B_2. The road length of the resulting link B_1–B_2 is set to the sum of the lengths of links B_1–A and A–B_2. The type of link B_1–B_2 is set to the worst of the types of the two original links (e.g., if the type of link B_1–A is HS highway and the type of link A–B_2 is primary road then the type of link B_1–B_2 is assigned as primary road). The capacity of link B_1–B_2 is set to the smallest of the capacities of links B_1–A and A–B_2 and the FFS is found from the capacity and the road type of link B_1–B_2. In the second case the link between nodes B_1 and B_2 is not created. We do not apply the above mechanism and keep nodes of degree 2 in the network when either of their two links is a ramp and the other one is not.

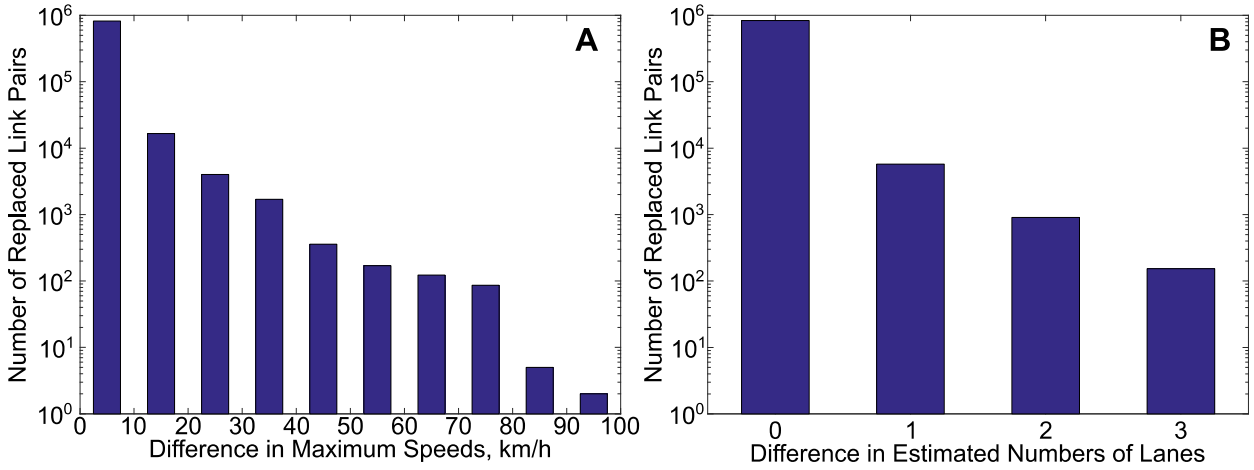

fig. S1. Effects of the removal of nodes of degree 2. Distribution of differences in estimated speeds (**A**) and numbers of lanes (**B**) between two roads connected to these nodes. Of 842 115 such link pairs in all 40 urban areas, 819 106 (97%) pairs had speed differences between links of 10 km/h or less, and 835 305 (99%) pairs had no differences in the estimated numbers of lanes.

Population assignment algorithm

In table S2 we describe the ESRI ArcMap tools we used to evaluate the number of people served by each of the intersections.

table S2. The algorithm of the node population assignment.

	ArcMap Tools	Description
1	Minimum Bounding Geometry	Build the minimum convex bounding polygon enclosing all nodes in the network.
2	Buffer	Create the buffer polygon around the nodes bounding polygon. The resulting buffer polygon may be defined as the union of the boundary polygon and all points within a certain distance from this polygon. In our study, the buffer distance was taken to be 1 mile.
3	Create Thiessen Polygons	Build Voronoi polygons for all nodes. Each Voronoi polygon contains only a single point input feature. Any location within a Voronoi polygon is closer to its associated point than to any other point input feature.
4	Clip	Clip Voronoi polygons with the buffer polygon.
5	Calculate Field	Calculate areas and population densities for all population distribution polygons.
6	Tabulate Intersection	Calculate the spatial composition of each of the Voronoi polygons in terms of population distribution polygons and calculate the population density of Voronoi polygons.
7	Calculate Field	Multiply the area of Voronoi polygons by their population density to evaluate the number of people. Assign this number as the population served by a node.

Distance factor of the likelihood of travel between nodes

To evaluate the trip distance factor $P(x_{od})$ we rely on 2009 survey data provided by the National Household Travel Survey (NHTS) (*55*, *56*). Overall, the resulting dataset contains data for all 150 147 completed households. As part of the survey, the queried households were asked to record parameters of their daily trips, such as distance travelled, on a certain day of the year.

We approximated the NHTS data with a piecewise continuous function. Let x be the distance between the origin and destination. The first two segments (for $x \in (0; 0.5]$ and for $x \in (0.5; 2.5]$) were chosen to be linear. The first segment was chosen to be a straight line connecting the point (0, 0) and the first bin point. The second segment was chosen to be a straight line connecting the last point of the first segment and the first point of the third segment.

For the third segment ($x \in (2.5; 34.5]$), we considered a polynomial model ($P(x) = k_3 x^{-b}$) and an exponential model ($P(x) = k_3 e^{-bx}$). As we observed a slightly better correlation between the model and the data with the exponential model, we used that model.

In table S3 we provide the precise definition of the distance factor $P(x_{od})$ of the likelihood of travel between nodes.

table S3. Distance factor $P(x_{od})$ of the likelihood of travel between nodes.

Function	Parameters		Argument (x_{od}) values (miles)	
	k	b		
0				0
$kd + b$	0.21995	0	0	0.5
$kd + b$	0.01188	0.10404	0.5	2.5
ke^{-bd}	0.21128	0.18296	2.5	34.5
0			34.5	

Estimation of the traffic speed from the density of vehicles

We employ a simple car following model to find the relationship between vehicles density and their macroscopic speeds.

Consider a network link, representing a road segment of length l with m lanes. Let D be the density of vehicles per unit length per one lane of the link. We assume uniform distribution of vehicles across the road segment. Then, on the whole link, the total number of vehicles N is

$$N = \frac{lm}{D} \tag{S1}$$

On the other hand, the density D equals the reciprocal average length of the road occupied by a single vehicle l_1: $D = 1 / l_1$. We assume that l_1 is composed of two parts the distance the driver needs to keep between their vehicle and the vehicle directly ahead and the vehicle size correction l_{veh}. We approximate the distance between two vehicles according to the two-second rule. This rule recommends that under normal road and weather conditions drivers keep the distance they cover in 2 seconds between their vehicle and the one they are following. Let t_r equal 2 seconds and v be the current traffic speed. Then

$$D = (l_{veh} + vt_r)^{-1} \tag{S2}$$

We assume that v is limited from the top at the free-flow speed V, which equals the speed limit set on the link. Then

$$v = \begin{cases} V, & \text{if } D \le D_c \\ \dfrac{1}{Dt_r} - v_{veh}, & \text{if } D_c < D \le D_{jam} \\ 0, & \text{otherwise} \end{cases} \tag{S3}$$

Above, $v_{veh} = l_{veh} / t_r$. $Dc = (l_{veh} + Vt_r)^{-1}$, and $D_{jam} = 1 / l_{veh}$. The fundamental traffic relationship between flow q, speed v, and density D is

$$q = Dv \tag{S4}$$

Using the relationship, we may express the traffic flow in terms of density as follows

$$q = \begin{cases} DV, & \text{if } 0 < D \le D_c \\ \dfrac{1}{t_r} - Dv_{veh} & \text{if } D_c < D \le D_{jam} \\ 0 & \text{otherwise} \end{cases} \tag{S5}$$

If we set $q_c = 1 / t_r$, we obtain the dependency shown in fig. S2 which represents the Daganzo traffic model (*59*).

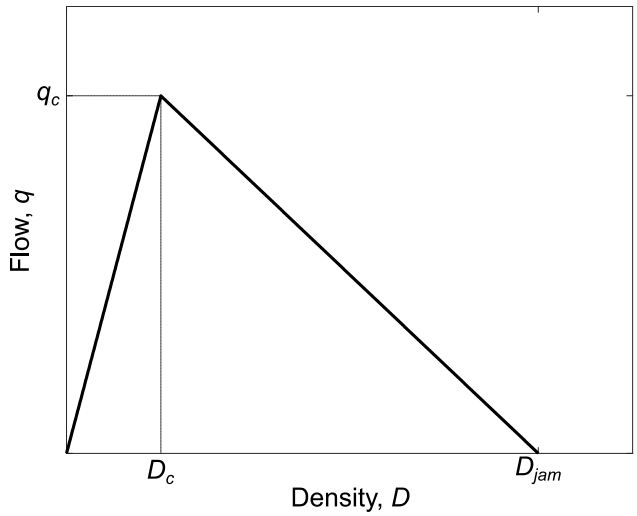

fig. S2. Density-flow relationship in the Daganzo traffic model.

Using equations (S1) and (S3) we find that for $D_c < D \leq D_{jam}$

$$v = \frac{lm}{Nt_r} - v_{veh} \tag{S6}$$

For a link, we approximate the number of vehicles N to be linearly proportional to the load L with the proportionality coefficient α

$$N = \frac{L}{\alpha} \tag{S7}$$

In addition, we assume that the minimum traffic speed is limited at a certain value v_{min}. This leads to Eq. (6) from the main text

$$v_{ij} = \alpha \frac{l_{ij} m_{ij}}{L_{ij}} - v_{veh}, \text{subject to } v_{ij} \in [v_{min}, V_{ij}] \tag{S8}$$

We assume l_{veh} to be 5 meters, giving v_{veh} = 9 km/h, while v_{min} is approximated to be the walking speed of 5 km/h.

Model calibration procedure

We calibrate the model to determine the value of α to match the real data on the annual average delay per peak-hour auto commuter provided by the Urban Mobility Scorecard (*11*). We use the delays data for 2010 as our census data are for that year. We search for parameter α maximizing the correlation between the modeled and actual delay times in representative 20 urban areas. To this end, we vary the value of the parameter α in the range of [200; 200,000] with the step of 200. We first divide the value of total delay ΔT (Eq. (5)) over the UA number of auto commuters (Urban Mobility Scorecard (*11*)). Then, we determine the proportionality coefficient β which minimizes the R-squared coefficient for the predicted and observed values assuming a simple linear dependency between these values passing through the point (0, 0).

We have found that for the 20 urban areas used for calibration R-squared coefficient took values in the range [-0.01; 0.83] (fig. S3). This allowed us to set $\alpha = 4.30 \cdot 10^4$ hour^{-1}, which corresponds to β of 10.59, and the Pearson coefficient of 0.91 ($p = 2.17 \cdot 10^{-8}$).

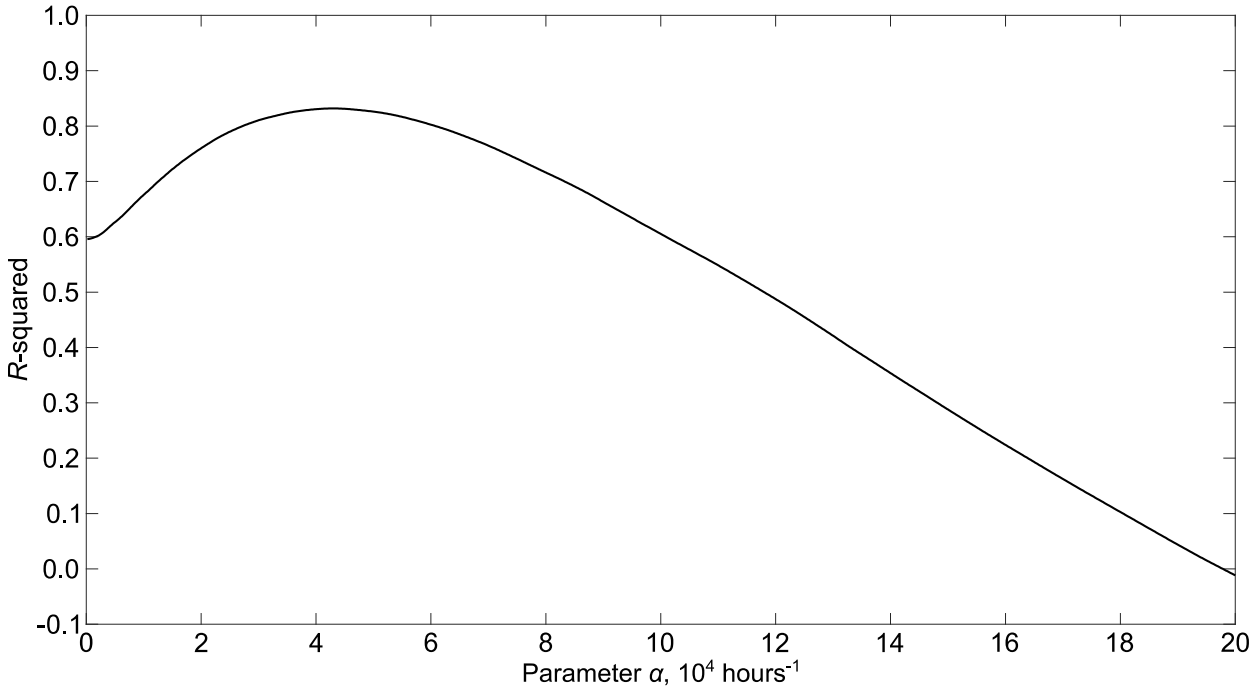

fig. S3. Model calibration. Optimization landscape showing dependency of R-squared correlation coefficient model for efficiency on the parameter α in Eqs. (6) and (S9).

Sensitivity of the model to ramp speeds

As outlined in the first subsection of Supplementary Materials, when the exact value of ramp speed is not available from data, we evaluate this value as a fraction of the average speed of the respective roadways (e.g., motorway ramp speed is a fraction of the average motorway speed). Let us further refer to this fraction as the ramp speed coefficient. In this subsection, we describe the study of the effect this coefficient has on delays and the correlation between the observed and modeled values.

All results and calculations presented in the manuscript were created using the ramp speed coefficient of 1/3. To validate that the model is stable for different values of the coefficient we consider 5 additional cases with ramp coefficient taking values from 0.3 to 0.7 with the step of 0.1. Figure S4 compares the observed and modeled delays for two values of the ramp speed coefficient: 1/3 and 1/2. Overall, we observe, that changing the coefficient may both increase and decrease the modeled delay. Yet, we note, that in any case the change is not significant. In addition, from the inset of fig. S4 we conclude that the Pearson correlation coefficient R between the observed and predicted values of delays does not change noticeably. We report the optimal fitting parameters α and β and the Pearson correlation coefficient for all values of the ramp speed coefficient in table S4.

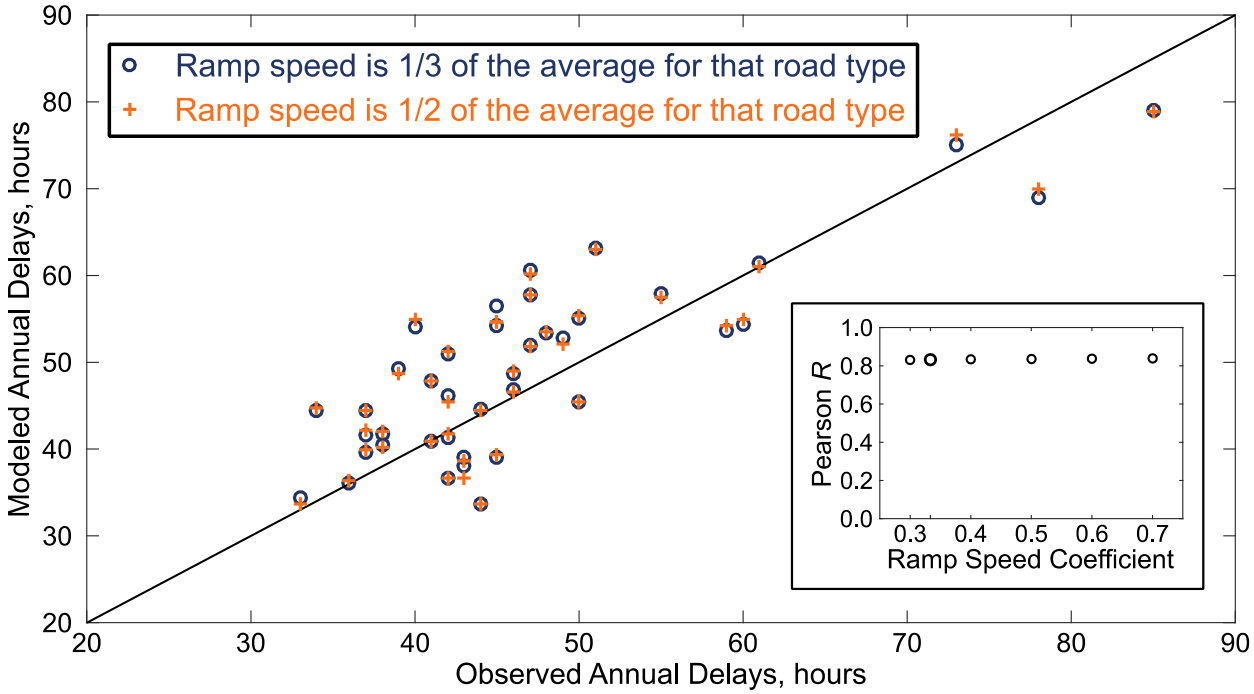

fig. S4. Modeled delays for ramp speed coefficients of 1/3 and 1/2. Increased estimated speed along ramps may both increase and decrease the predicted delays. However, in all cases the changes are negligible. The inset implies that the Pearson correlation coefficient R does not change significantly with the ramp speed coefficient.

table S4. Model sensitivity to ramp speed coefficient. The coefficient of 1/3 is used in the study. Pearson *R* is provided for all 40 areas used for calibration and validation.

Ramp speed coefficient	Parameter α	Parameter β	Pearson *R*
0.3	42 600	10.5639	0.8311
1/3	**43 000**	**10.5898**	**0.8322**
0.4	44 800	10.7238	0.8334
0.5	45 800	10.7567	0.8358
0.6	46 600	10.7701	0.8375
0.7	47 200	10.7697	0.8382

Additional delay as a function of the severity of link disruption

We present the results of delay times in all 40 urban areas for the full spectrum of adverse event severities, $r \in [0; 1]$ in fig. S5 (compare to Fig. 5 in the main text which shows the results for only 6 representative urban areas).

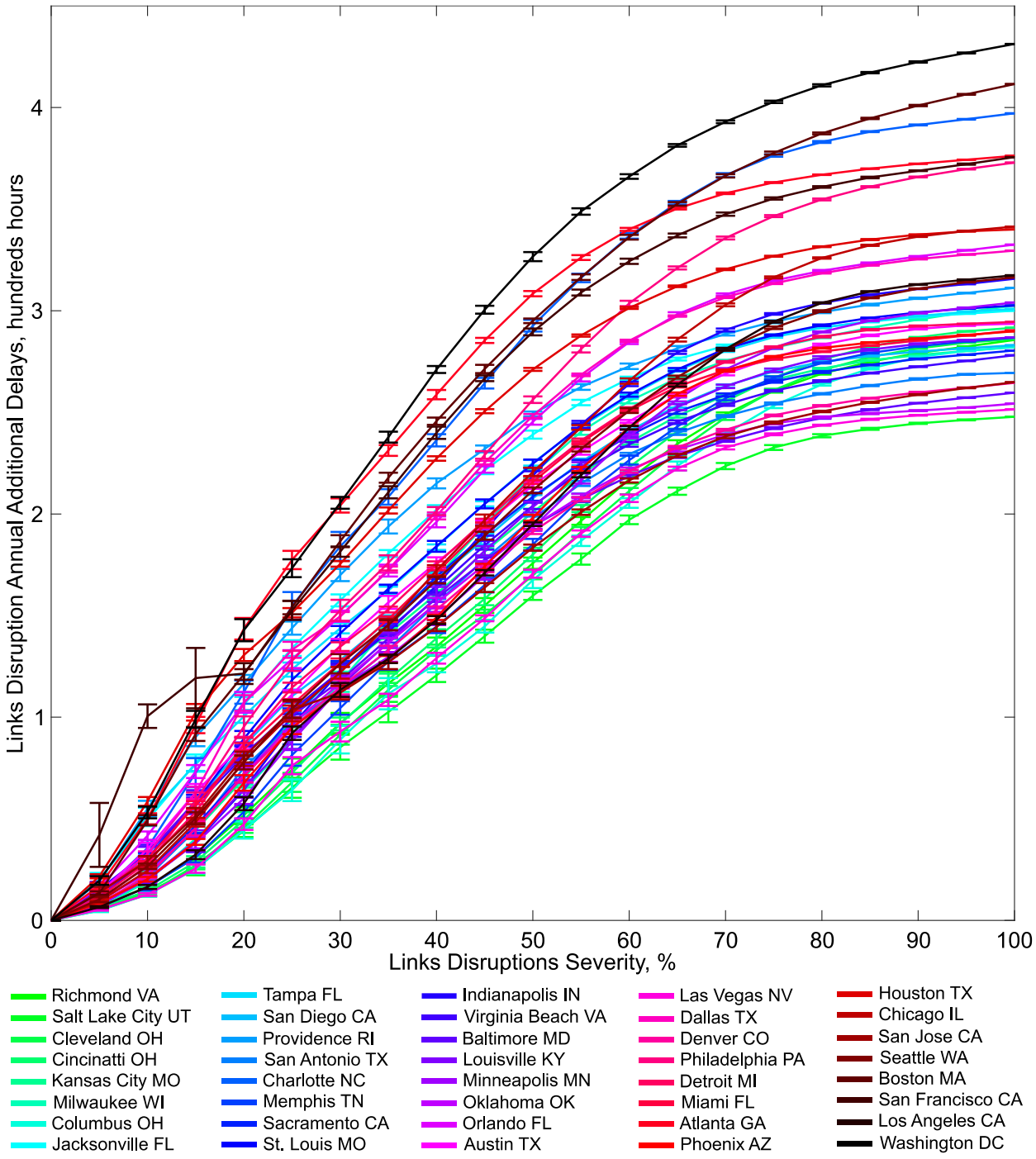

fig. S5. Dependency of the additional delay on the severity of the link disruption for all 40 urban areas. Error bars show mean values ± standard deviation. Cities are ordered by the observed delays.